Civil and Environmental Engineering
Vol. 20, Issue 2, 632-653, DOI: 10.2478/cee-2024-0048

INELASTIC MOMENT RESISTANCES OF WELDED STEEL BEAMS WITH INITIAL SHAPE IMPERFECTIONS

Phe VAN PHAM[1,*], Thi DOAN-TAN[2], DUNG LE-DANG[3], Nguyen XUAN-Huy[3]

[1] Faculty of Civil Engineering, University of Transport and Communications, #3 Cau Giay, Hanoi, Vietnam.
[2] Ph.D. Candidate, Faculty of Civil Engineering, Campus in Ho Chi Minh City, University of Transport and Communications, # 450- 451 Le Van Viet, Ho Chi Minh City, Vietnam.
[3] Faculty of Construction Engineering, University of Transport and Communications, #3 Cau Giay, Hanoi, Vietnam.
* corresponding author: phe.phamvan@utc.edu.vn

Abstract

Numerical procedures based on geometric and material nonlinearities are proposed in the present study to evaluate the inelastic responses of welded steel beams with the initial shape imperfections of welds, braces and out-of-straightness. The convergent deformations/moments of the present solutions are excellently validated against experimental results. Thirty-seven steel beams with different sectional classes are then proposed to quantify the effects of initial shape imperfections of welds, braces, and out-of-straightness on the system deformations and moment resistances. It is observed from the present study that the moment resistances strongly depend on the residual stresses, bracing heights, and out-of-straightness shapes for the beams with compact and non-compact sections, but they are insensitive for the beams with slender sections. The effects of weld shapes on the moment resistances are found to be small. Through an evaluation of the moment resistances of typical design specifications, design considerations are proposed for the steel beams subjected to the initial imperfection shapes.

Keywords:

Inelastic LTB moments;
Imperfections;
Weld shapes;
Residual stresses;
Bracing heights;
Initial out-of-straightness shapes.

1. Introduction and Motivations

Steel beams are widely installed in various civil structures, such as bridges, buildings and ports. Most countries have their own specifications for the design of the beams (e.g., [1,2]). Although there are strict requirements for the design of moment resistances of such structures, there may be potential defects those have not been specified by the design and they may lead to unforeseen failures of the structures (e.g., [3,4,5,6,7]). One of the concerns in the design is the impact of residual stresses caused by welding processes. While AISC [1] proposes simplified equations for the beams with a residual stress model based on rolled sections and the EC 3 [2] specification provides different design curves for rolled or welded cross-sections, the effect of residual stresses caused by different weld shape imperfections seems not to be covered by the design equations. Also, in the installation stage of a slab-steel composite beam, the steel beam is often kept in place by using temporary discrete lateral brace points (or cross beams) before being attached with a top slab by stubs to generate a continuous bracing system. However, the condition of different bracing heights may influence on the resistances of the beams. There were structural failures in such scenarios (e.g., [4-7]). For civil structures in operation stages, we may also meet steel beams having their webs discretely braced, but the brace heights are partially reduced by corrosions/connection lost, those may also influence on the moment resistances of the system. The thus discussed effects of residual stresses and bracing conditions on the moment resistances of steel beams may be more severe with the additional joining of the initial beam out-of-straightness. The initial out-of-straightness are normally based on an assumption of single curvature of the beam (e.g., the first elastic lateral torsional buckling (LTB) mode) [1,2]. However, it may have a different shape with more curvatures (e.g., the second elastic LTB buckling mode). The moment resistance under the effect of the latter out-of-straightness shape may be different to that of the former one and this needs to be clarified. To investigate the effects of such three important initial imperfections on the design of the moment resistances of steel beams, there have been many studies conducted.

The residual stresses of welded I-beams often have relatively complicated distributions across the member thicknesses and widths, resulted from different welding processes [8,9,10,11,12,13]. Kabir and Bhowmick [14] and Rossi et al. [15] adopted three simplified residual stress models of welded structures to numerically investigate the LTB moment resistances of I-weld steel beams. However, their residual stress models were taken from the simplified models of Taras [16] for mill plate cut sections, Barth and While [17] for flame cut sections, and EC 3 [2] for approximate models, as depicted in Fig. 1a,b,c. Subramanian and White [18] and Boissonnade and Sonja [19] numerically studied the effects of mill-cut and flange-cut – based residual stresses (Fig. 1a,b) on the LTB moment resistances of steel I beams with slender flanges and non-compact webs. The authors found that the LTB moment resistances based on numerical analyses were lower than those of experimental results. Le et al. [20] conducted experimental and numerical studies on the LTB moment resistances of welded high strength steel I-beams with compact and non-compact sections. The residual stresses in [20] were measured by using a laser scanning and they are adjusted to fit a simplified model as depicted in Fig. 1a. The weld shapes of all specimens in [20] were taken as a linear line (as depicted in Fig. 2b1) with a single pass of 6.0mm. Trahair et al. [21], Trahair [22], Kubo and Fukomoto [23], Nishino et al. [24], Baker and Kennedy [25], Ziemian [26], Abebe et al. [27], Kennedy and Aly [28], White et al. [29] presented simplified theoretical solutions for the buckling responses of beams and columns under the effects of residual stresses. Recently, Couto and Real [30] conducted numerical studies for the investigation of local buckling responses of welded I beams with slender webs/flanges. However, their numerical models were meshed by shell elements and their residual stress model was taken from previous studies. Such treatments ignored the welds because they could not be created by such a modeling. Also, the distribution of residual stresses across the member thicknesses were not considered in their studies [30,31]. It can be summarized from the previous studies [14-30] that their residual stress models have not considered the effects of weld shapes and welding processes. Also, the LTB resistances of the structures in studies [14-30] were based on simplified residual stress models, in which the residual stresses were assumed as a constant across the member thicknesses.

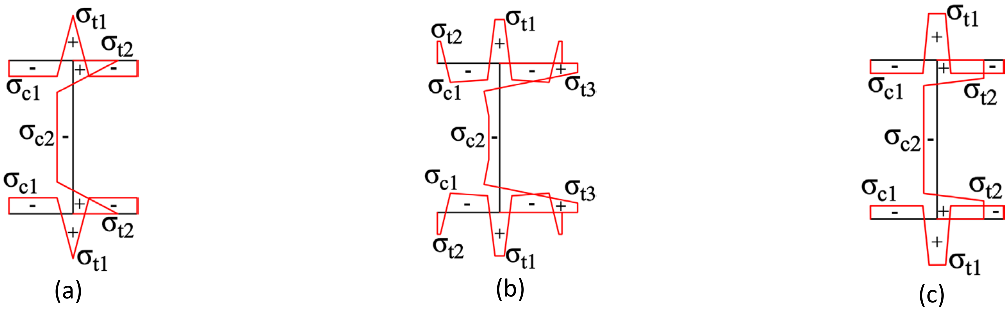

Fig. 1: Typical simplified residual stress models in welded steel sections (a) mill cut [8,9,16], (b) flame cut [9,11,17], and (c) approximate model [1,8-12,13]

During construction or operation stages, the moment resistances of steel beams with discrete braces attached to the sectional webs have strongly depended on the unbraced beam lengths [1,2,3,5]. Such a brace can work to resist the lateral displacement and/or twisting angle of the braced cross-section [1]. There were studies on effects of such bracing conditions on the responses of steel members. Pezeshky et al. [32] indicated that the effects of bracing heights on the elastic LTB moment resistances of I steel beams were significant. They proposed three 1-dimensional finite element formulations to evaluate the elastic resistances of steel beams with five different bracing conditions (i.e., top flange braced, bottom flange braced, section centroid braced, top and bottom flanges braced, and no bracing). However, the study [32] only focused on the elastic LTB responses and the heights (or depths) of cross braces were not considered in their solutions. Dou and Pi [33] and Kortis et al. [34] numerically investigated the effects of elastically deformable discrete braces on the flexural buckling resistances of steel columns/trusses under axial loads. Gocal et al. [35] performed an experimental analysis of the bracing stiffness effects on the normal stresses of the bridge deck members. Canh et al. [36,37,38] developed analytical solutions for the elastic lateral torsional buckling, elastic flexural torsional buckling, and free vibrations of steel beams with different bracing systems attached to the beam webs (i.e., cross beams, floor beams and cross frames). Foster and Gardner [39] conducted experimental and numerical investigations of the LTB moment resistances of continuous steel beams with rigid and elastically deformable lateral braces. Mohammadi et al. [40] developed a finite element formulation for the prediction of the elastic LTB moments of I beams with variable torsional bracing stiffnesses. Nakamura [41] and Tong and Chen [42] developed simplified solutions for the lateral and torsional stiffnesses of lateral braces in steel beams with discrete braces. As revised from above works, it can be observed that the studies (i.e., [32-42]) did not considered the effects of the lateral brace heights on the inelastic LTB deformations/ moment resistances of steel beams. In fact, a cross brace fully attached along the whole depth of the web may ensures that the braced cross-section is completely restrained against both of the lateral and twisting deformations [20]. However, there are other scenarios that the full bracing condition is not achieved (e.g., incomplete brace installation in construction stages, the connection of the cross brace and the steel web may be partially lost or corroded [3,5,7]), those can change the system deformations and reduce the beam moment resistances. A further investigation for the moment resistances of the steel beams under such partial bracing heights may be necessary to propose design considerations for structural engineers.

In most numerical and experimental studies on the effects of initial imperfections on the (inelastic) LTB moment resistances of steel beams, residual stresses are often considered in conjunction with initial out-of-straightness of the beams. While AISC [1] had a requirement for the maximum out-of-straightness of the beam axis is $L_u/1000$ (where L_u is the unbraced length of the beam), EC 3 [2] proposed several simplified solutions for different levels of initial out-of-straightness based on rolled or welded sections and the ratio of sectional height and width. Dou and Pi [32] numerically investigated the effects of different shapes of initial out-of-straightness on the flexural torsional buckling of steel columns under compressions. The imperfection shapes of the beams considered in [32] were based on the first, the second, the third or mixed elastic LTB modes. Boissonnade and Sonja [19] studied the effects of the initial out-of-straightness based on the first LTB mode and initial local imperfections of flanges and webs. Couto and Real [30] numerically investigated the effect of the initial local imperfections on the LTB moment resistances of steel beams. The consideration of the initial out-of-straightness based on the first LTB mode in the nonlinear analyses of steel beams was also included in the works of Abebe et al. [27], Phe and Huy ([43], Phe [44], Vales and Stan [31], Bachiri et al. [45], and Le et al. [20], and Kabir and Bhowmick [14], and Yi et al. [46]. It can be observed from the studies that they only considered the initial out of straightness based on the first LTB mode or local imperfections of the flange and webs. The study of Dou and Pi [32] also considered the imperfection based on the second and third modes, however it was restricted for column structures under axial loads. As discussed, the initial out-of-straightness of the beams may be based on a single curvature of the beam (e.g., the first elastic lateral torsional buckling (LTB) mode) or it may have a different shape with more curvatures (e.g., the second elastic LTB buckling mode). The moment resistances of steel beams under the effect of the latter out-of-straightness shape may be different to those of the former one and this has not fully been investigated in the previous studies.

Based on the thus discussed shortcomings of the previous studies [1-46], the present work is motivated to perform a study on the effects of the initial shape imperfections of welds, braces and out-of-straightness on the moment resistances of steel beams. The residual stresses obtained from different weld shapes (including linear, concave, convex, mixed welds) and from a welding process (including heating, heat maintaining and cooling times) will be developed in the present study. Different bracing heights and out-of-straightness shapes will be also considered in a combination with the residual stresses. In the present study, the effects of the initial imperfections on the inelastic LTB moment resistances of the steel beams with different section classifications will be investigated, quantified and checked against the design results based on typical specifications for steel structures [1,2]. Design considerations/recommendations for the beams under such imperfections will be subsequently proposed. Because the analyses of residual stresses, elastic and inelastic LTB moment resistances and deformations of the beams in the present study will depend on nonlinear geometries and/or materials, they will be numerically conducted by using a finite element (FE) simulation package. Because most FE packages have not had guides for the analysis of the inelastic LTB moment resistances of the steel beams with such initial imperfections, the present study will propose a completely numerical modelling procedure to successfully obtain the nonlinear responses of the problem.

2 Scope of the present study

In the present study, simply supported beams with four cross braces at Points *A*, *B*, *C*, and *D* and with a wide flange section are proposed for the investigations (Fig. 2a,b). The distance between support *A* and Point *B* or Point *C* and support *D* is L_1, while the distance between Point *B* and Point *C* is L_0. The beam cross-sections considered in the present study include compact, non-compact and slender sections based on AISC [1] (corresponding to classes 1, 2, 3, 4 based on EC 3 [2]). The beams are subject to two point loads P transversely applied at *B* and *C*. The beam is subjected to three types of initial imperfections. First, the cross-section is built by using four fillet welds those have a toe width of t_{we} and a toe height of h_{we} (Fig. 2b). Four different shapes including linear welds (Fig. 2b1), concave welds (Fig. 2b2), convex welds (Fig. 2b3), mixed welds (Fig. 2b4) are considered. Second, the lateral bracing height at Points *B* and *C* is h_{br} that can be varied but symmetrical about the sectional centroid O (Fig. 2c). And third, the beam is subjected to different modes of initial out-of-straightness (e.g., Fig. 2d1, d2). Under such imperfections, the moment resistances of the structures will be completely evaluated by numerical procedures. The resistances evaluated by using typical specifications including AISC [1], EC 3 [2] will be also reviewed and design considerations will be proposed.

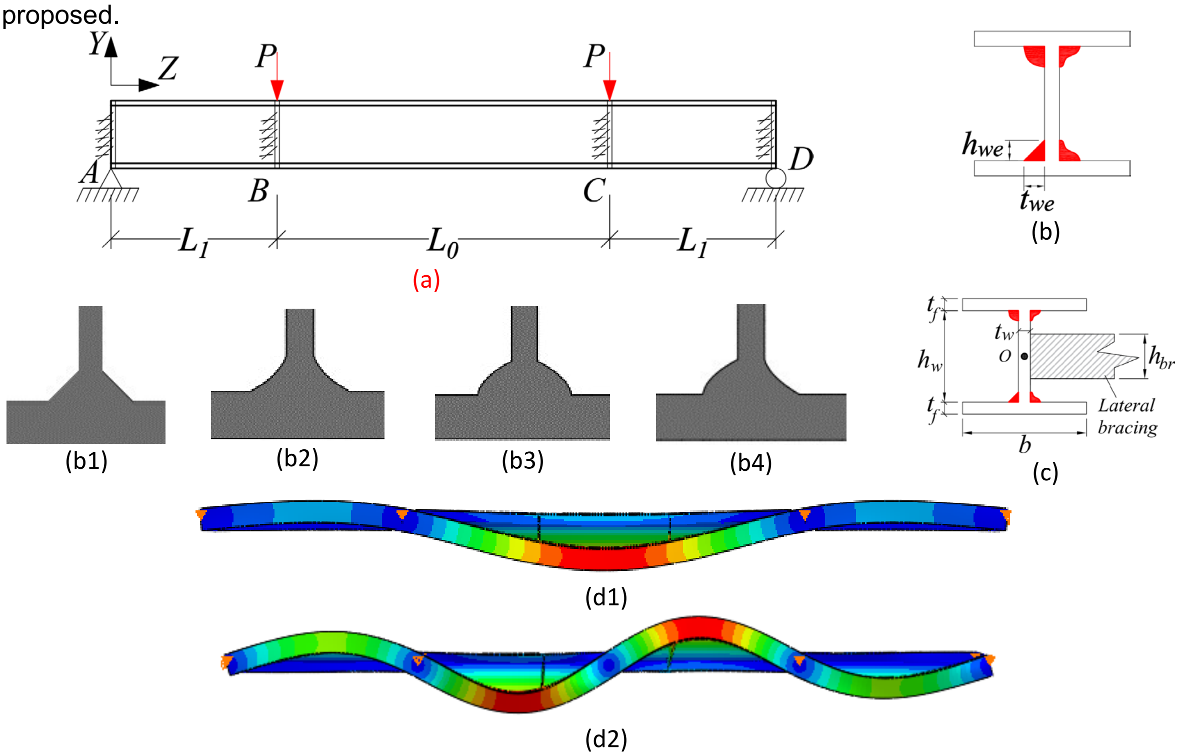

Fig. 2: Definition of the beams with initial imperfections considered in this study (a) beam profile, (b) welds, (b1, b2, b3, b4) linear, concave, convex, and mixed weld shapes, (c) cross-sectional dimensions and cross bracing configurations, and (d1, d2) Magnified initial out-of-straightness shapes

In order to conduct the numerical solutions, dimensions and material properties of the structures are defined. The span lengths of the beams are assumed as $L_1 = 1.5\,m$ and $L_0 = 3.0\,m$, while four different cross-sections CS1, CS2, CS3 and CS4 based on compact, non-compact and slender classifications [1] or classes 1,2,3,4 [2] are given in Table 1. Thirty seven cases of steel beams, denoted as SS00 through SS36, with different sectional classes and with different initial imperfections of braces, residual stresses and out-of-straightness are proposed in Table 2. In which Cases SS00 through SS12 are the beams with the CS3 cross-section (i.e., compact sections), while Cases SS13 to SS20 are those with the CS1 (i.e., non-compact flange and compact web), Cases SS21 to SS28 are those with the CS2 (i.e., non-compact flange and compact web), Cases SS29 to SS36 are those with the CS4 (i.e., slender flange and slender web).

Table 1: Beam cross-section types considered in the present study

Cross-section symbol	**Description of section classification**		h_w	t_w	b	t_f
	AISC [1]	**EC 3 [2]**				
CS1	Compact Web, Compact Flange	Class 1	330	10	160	14
CS2	Compact Web, Noncompact Flange	Class 2	330	8	160	12
CS3	Compact Web, Noncompact Flange	Class 3	330	7.7	160	12
CS4	Slender Web, Slender Flange	Class 4	330	3.4	160	6

In Table 2, four absolutely rigid bracing scenarios denoted as BS1, BS2, BS3 and BS4 have been defined, in which BS1 is the case that the clear web depth of the section is fully braced at B and D (i.e., $h_{br} = h_w - 2h_{we}$, Fig. 2b,c), BS2 is the case that a half of the web depth is braced at B and D (i.e., $h_{br} = h_w / 2$), BS3 is the case that the one-fourth web depth is braced at B and D (i.e., $h_{br} = h_w / 4$), and BS4 is the case that the one-eighth web depth is braced at B and D (i.e., $h_{br} = h_w / 8$). Also, four different weld shapes denoted as ReS1, ReS2, ReS3, and ReS4 have been considered, in which the ReS1 has a linear shape (Fig. 2b1), the ReS2 has a concave shape (Fig.2b2), the ReS3 has a convex shape (Fig. 2b3) and the ReS4 has a mixed shape (Fig. 2b4). All welds have the dimensions of $h_{we} = t_{we} = 6.0\,mm$. The initial beam out-of-straightness shapes have been also defined Table 2 and they are the first and the second elastic LTB modes with a maximum deformation of $L_0 / 1000$ (Figs. 2d1,d2), in which the first mode is symbolled as IMM1 while the second one is IMM2.

Steel materials at room temperature are assumed to have a modulus of elasticity of $210\,GPa$ and a Poisson's ratio of 0.3, and a perfectly plastic strength of $690\ MPa$ [20,47]. The properties are dependent on temperatures in the welding process and they will be defined in the welding section below.

Table 2: Steel beams with different conditions of welds, braces, and initial out-of-straightness

Beam #	Cross-section	Bracing system	Residual stresses	Initial out-of-straightness
SS00	CS3	BS1	N/A	N/A
SS01			ReS1	N/A
SS02			ReS1	IMM1
SS03			ReS1	IMM2
SS04			ReS2	IMM1
SS05			ReS3	IMM1
SS06			ReS4	IMM1
SS07		BS2	ReS1	IMM1
SS08				IMM2
SS09		BS3	ReS1	IMM1
SS10				IMM2
SS11		BS4	ReS1	IMM1
SS12				IMM2
SS13	CS1	BS1	ReS1	IMM1
SS14				IMM2
SS15		BS2	ReS1	IMM1
SS16				IMM2
SS17		BS3	ReS1	IMM1
SS18				IMM2
SS19		BS4	ReS1	IMM1
SS20				IMM2
SS21	CS2	BS1	ReS1	IMM1
SS22				IMM2
SS23		BS2	ReS1	IMM1
SS24				IMM2
SS25		BS3	ReS1	IMM1
SS26				IMM2
SS27		BS4	ReS1	IMM1
SS28				IMM2
SS29	CS4	BS1	ReS1	IMM1
SS30				IMM2
SS31		BS2	ReS1	IMM1
SS32				IMM2
SS33		BS3	ReS1	IMM1
SS34				IMM2
SS35		BS4	ReS1	IMM1
SS36				IMM2

3 Description of the present solutions based on a complete modelling procedure

3.1 A complete modelling procedure of the beams

The well-known finite element analyses package ABAQUS is selected for the numerical solutions conducted in the present study. Although there are one- or two- dimensional elements available in the package library, they may not be suitable for the modelling. Because the fillet welds and the residual stresses varied across the member thicknesses may not be captured by the models meshed by such elements. In order to generate the residual stresses through a welding process as well as to input the initial bracing and out-of-straightness conditions, three-dimensional elements are proposed for the present finite element modelling. Three types of analyses, denoted as FEA-Types 1, 2, 3, are proposed to completely model the structures under the effects of the initial imperfections and they are defined in the following.

FEA-Type 1: A nonlinear coupled temperature - displacement analysis of the structure under welding heating and cooling stages to obtain residual stresses.

FEA-Type 2: An elastic buckling analysis to obtain the initial out-of-straightness shapes through the adjustment of the first and second lateral torsional buckling modes.

FEA-Type 3: A nonlinear plasticization analysis to obtain the inelastic LTB deformations and moment resistances of the systems under the effects of different conditions of braces, residual stresses (taken from FEA-Type 1), and initial out-of-straightness (taken from FEA-Type 2).

3.1.1. Generation of a finite element mesh

In the three analyses above, the flanges and the web of the steel beams all are meshed by cubic C3D8RT elements (in FEA-Type 1) or C3D8R elements (in FEA-Types 2 and 3), while the welds are meshed by both cubic C3D8RT and wedge C3D6T elements (in FEA-Type 1) or C3D8R and C3D6 elements (in FEA-Types 2 and 3). Such a mesh is controlled by 18 independent numbers of elements along different edges, as described in Fig. 3a,d. In the cross-sectional view (Fig. 3a), n_{11} and n_{22} are the numbers of elements across the flange overhang (having a width of $(b-t_w)/2-t_{we}$ and excluding the weld width t_{we}), n_{12} and n_{21} are those across the weld width t_{we}, n_3 is that across the flange thickness, n_{41} and n_{43} are those across the weld height h_{we}, n_{42} is that across the web height excluding the weld heights. In the axial direction (Fig. 3d), the beam span is divided into 11 segments with different lengths L_{5i} and numbers of elements n_{5i}, $i=1,2,...,11$. Web stiffeners, lateral braces and/or loads will be added in segments L_{51}, L_{53}, L_{55}, L_{57}, L_{59} and L_{511}, those are meshed by the numbers of elements n_{51}, n_{53}, n_{55}, n_{57}, n_{59} and n_{511}. The segments without stiffeners, braces or loads are L_{52}, L_{54}, L_{56}, L_{58} and L_{510} those are meshed by coarser numbers of elements n_{52}, n_{54}, n_{56}, n_{58} and n_{510}.

For fillet welds, local coordinate systems $x_1O_1y_1$ are assumed, in which x_1 is the lateral axis, y_1 is the vertical axis, and O_1 is the origin (Fig. 3b,c). The linear, concave, or convex weld shapes can be respectively created by using functions $f_1(x_1,y_1)$, $f_2(x_1,y_1)$, $f_3(x_1,y_1)$ (Fig. 3b) those generate perpendicular distances at the mid points of the weld curves as $a_1 = 2.0\,mm$. Such shapes are approximately meshed by C3D8R and C3D6 elements, in which C3D6 elements are wedged at the boundary of the function $f(x_1,y_1)$ (Fig. 3c). The nodes and elements of such weld shapes can be separately done in spreadsheet .csv files and they are then inserted into ABAQUS input file through command keyword *INCLUDE, INPUT.

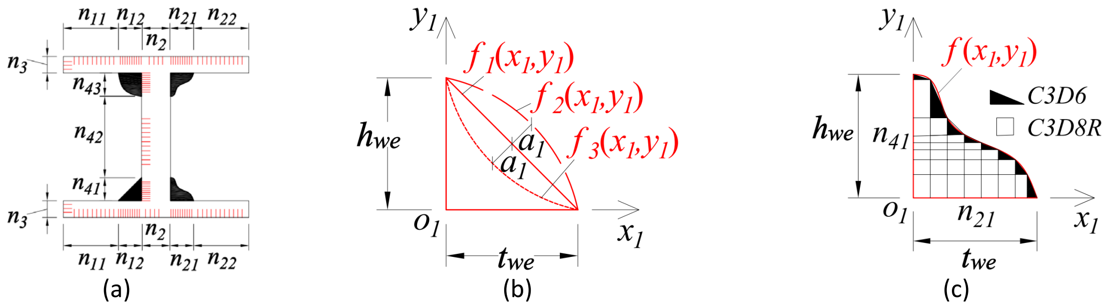

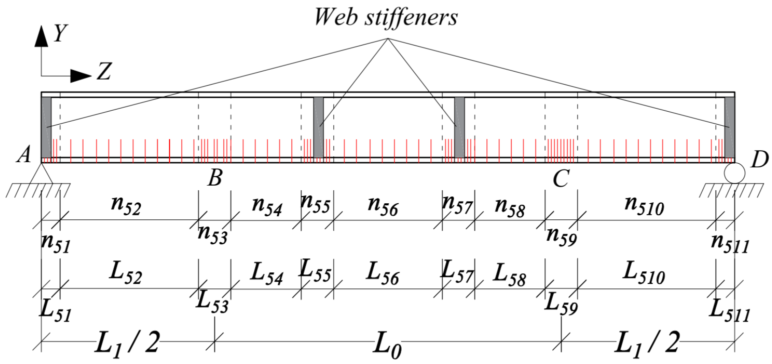

Fig. 3: Mesh generations in the present numerical model (a) cross-section, (b,c) weld geometry and mesh, and (d) profile view

3.1.2. Input of the residual stresses obtained from the FEA-Type 1 into the FEA-Type 3

The welding process experiences heating and cooling times. The material properties of steel depend on temperatures and they are defined in [8-11, 20]. The values of specific heat and thermal conductivity against temperature changes in the welds are given in [8-12, 20, 47]. The heating is from $20^o C$ to $1470^o C$ and it takes about 80 seconds, the peak temperature is maintained about 20 seconds, then the cooling is from $1470^o C$ to $20^o C$ and it is assumed to take place in 600 seconds. Based on such given data, a coupled temperature-displacement analysis is conducted in the FEA-Type 1 to obtain the residual stresses after the cooling time. Such residual stresses for ReS1, ReS2, ReS3, ReS4 weld shapes are obtained and their contours are depicted in Fig. 5a-e. As observed, the von Mises residual stresses distributions are not constant across the thicknesses of the flanges and web. Also, they are highly concentrated at the web and flange intersection zones while they are almost constant at other locations. The stress outputs are observed to relatively agree with the residual stress models of EC 3 specification [2] and the study of Le et al. [20]. The residual stresses of elements stored in the FEA-Type 1 are inputted into FEA-Type 3 through command *Initial Conditions, Type=STRESS.

Table 3: Thermal material properties of steel

$T(^0C)$	$\sigma_y(MPa)$	$E(MPa)$	μ	$\alpha\,(1/^o\,C)$
20	690	210000	0.3	1.3×10^{-5}
600	370	110000	0.3	1.6×10^{-5}
> 1000	20	10000	0.4	1.7×10^{-5}

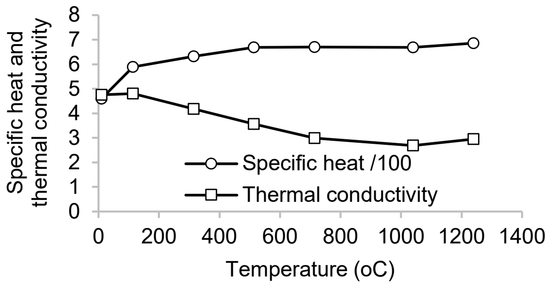

Fig. 4: Thermal properties of the welds

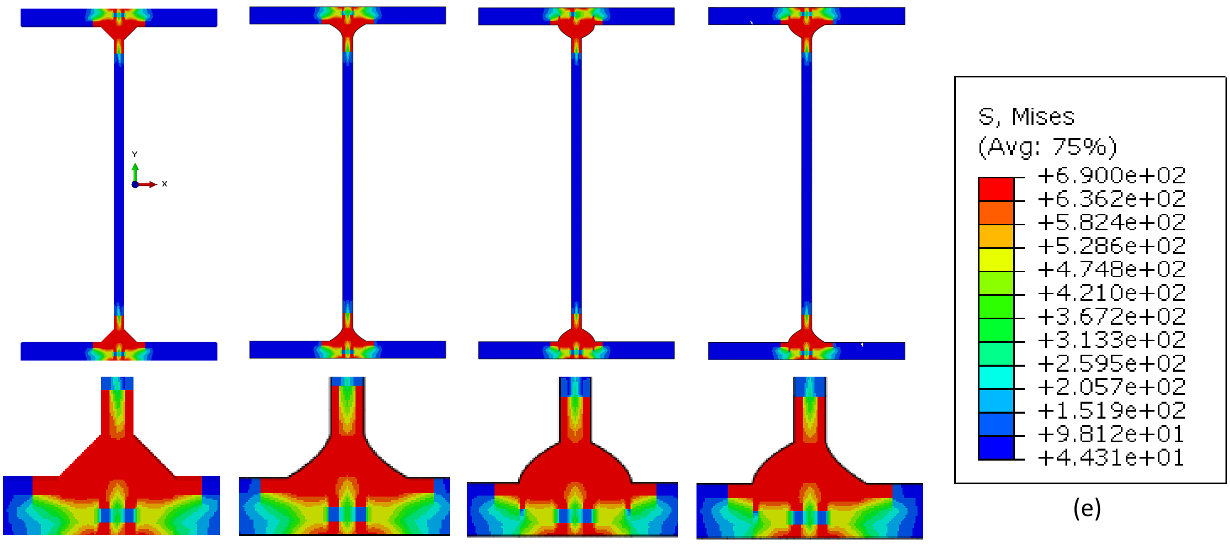

Fig. 5: Residual stress models in the numerical study (a) ReS1, (b) ReS2, (c) ReS3, (d) ReS4 and (e) stresses contour values

3.1.3. Input of lateral braces

In all types of analyses (i.e., FEA-Types 1, 2, 3), absolutely rigid lateral bracing conditions BS1, BS2, BS3 and BS4 at Points B and C may be created by applying displacement constraints in the lateral direction of the nodes lying on the vertically symmetric axis of the cross-sections at Points B and C of the beam, as depicted in Fig. 6a-d and Fig. 7a.

3.1.4. Input of the initial out-of-straightness obtained from FEA-Type 2 into FEA-Type 3

The analyses of elastic global buckling of the system are conducted in the FEA-Type 2 through command *buckle. The initial out-of-straightness of the beam is based on the first or the second lateral torsional buckling modes of the FEA-Type 2 with an maximum deformation of $L_0 / 1000$ (as defined in Figs. 2d1, d2). Then, such initial imperfections are inputted into the FEA-Type 3 through command *IMPERFECTION.

3.1.5. Obtaining the moment resistances in the FEA-Type 3 and a mesh sensitivity study:

After generating a mesh and inputting the initial imperfection shapes of braces, residual stresses and out-of-straightness, the FEA-Type 3 is nonlinearly analyzed by using Riks method through commands *STEP,NLGEOM=YES and *STATIC, RIKS. After completing the analysis, the data of applied loads (or reaction forces) and deflections can be extracted. Moment-deflection relationships can be thus deduced.

Because the FEA results depend on the element mesh, a mesh sensitivity is conducted to investigate the result convergences. Four different meshes in Table 4 are proposed for the study. Fig. 7a-k present an example of the structural modeling when Mesh 3 is adopted, in which Fig. 7a, b present the structural mesh in 3D and cross-sectional views, Fig. 7c is a magnified 3D view of bottom flange with line weld shape, Fig. 7d, e, f are the models with concave, convex and mixed weld shapes, Fig. 7g, i present the pin and movable supports at Points A and D, and Fig. 7h is a magnified view of the pin support in Fig. 7g, while Fig. 7h is a magnified view of the pin support in Fig. 7i.

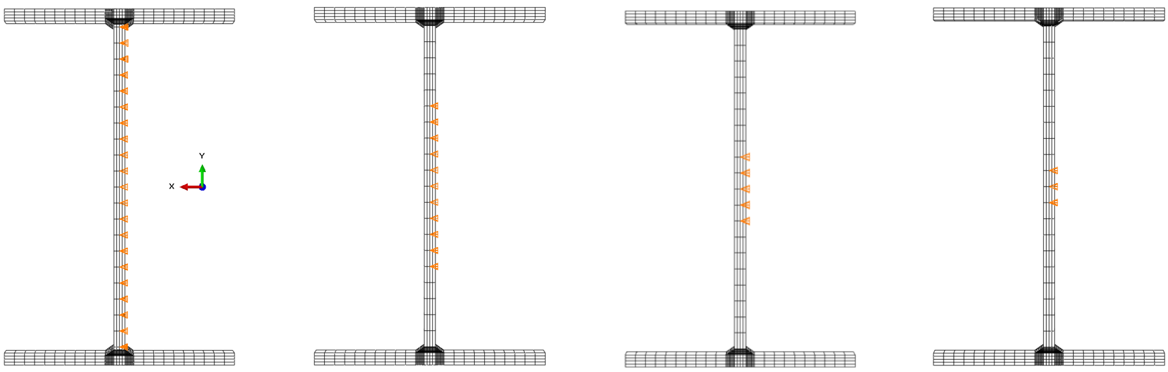

(a) (b) (c) (d)

Fig. 6: Lateral bracing conditions at Points B and C in the numerical solution (a) BS1, (b) BS2, (c) BS3 and (d) BS4

Table 4: Meshes proposed in the present FEA solutions

Mesh	n_{11}	n_{12}	n_2	n_3	n_{41}	n_{42}	n_{43}	n_{51}	n_{52}	n_{53}	n_{54}	n_{55}	n_{56}	n_{57}	n_{58}	n_{59}	n_{510}	n_{511}
1	4	4	2	2	4	4	4	4	10	4	10	4	10	4	10	4	10	4
2	8	6	4	4	6	10	6	8	20	8	20	8	20	8	20	8	20	8
3	10	10	4	4	10	20	10	8	40	8	40	8	40	8	40	8	40	8
4	20	20	4	4	20	40	20	8	80	8	80	8	80	8	80	8	80	8

The results of inelastic moment resistances M_n of Beams SS00 and SS02 obtained from the FEA-Type 3 with four meshes 1, 2, 3, 4 are considered and they are presented in Table 5. For each of the beams, the moment resistance based on Mesh 4 is taken as the reference value to compare against those of other meshes. For Beam SS00, the moment resistance based on Mesh 4 is 600.9 kN.m, while those of Meshes 1, 2, 3 are 528.1 kN.m, 592.5 kN.m, and 600.0 kN.m respectively, corresponding to the differences of 12.1%, 1.4% and 0.2%. For Beam SS02, the moment resistance of Mesh 4 is 505.1 kN.m, while those of Meshes 1, 2, 3 are 409.2 kN.m, 485.5 kN.m, and 504.0 kN.m respectively, corresponding to the differences of 19.0%, 3.9% and 0.2%. As observed, the results based on Mesh 3 are almost identical to those of Mesh 4, while Mesh 3 is coarser than Mesh 4. Therefore, Mesh 3 is selected for the numerical solutions in the present study.

Table 5: Moment resistances (kN.m) based on 4 meshes proposed in the present FEA solutions

Mesh	**Case SS00**		**Case SS02**	
	M_n	**% difference**	M_n	**% difference**
1	528.1	12.1	409.2	19.0
2	592.5	1.4	485.5	3.9
3	600.0	0.2	504.0	0.2
4	600.9	0.0	505.1	0.0

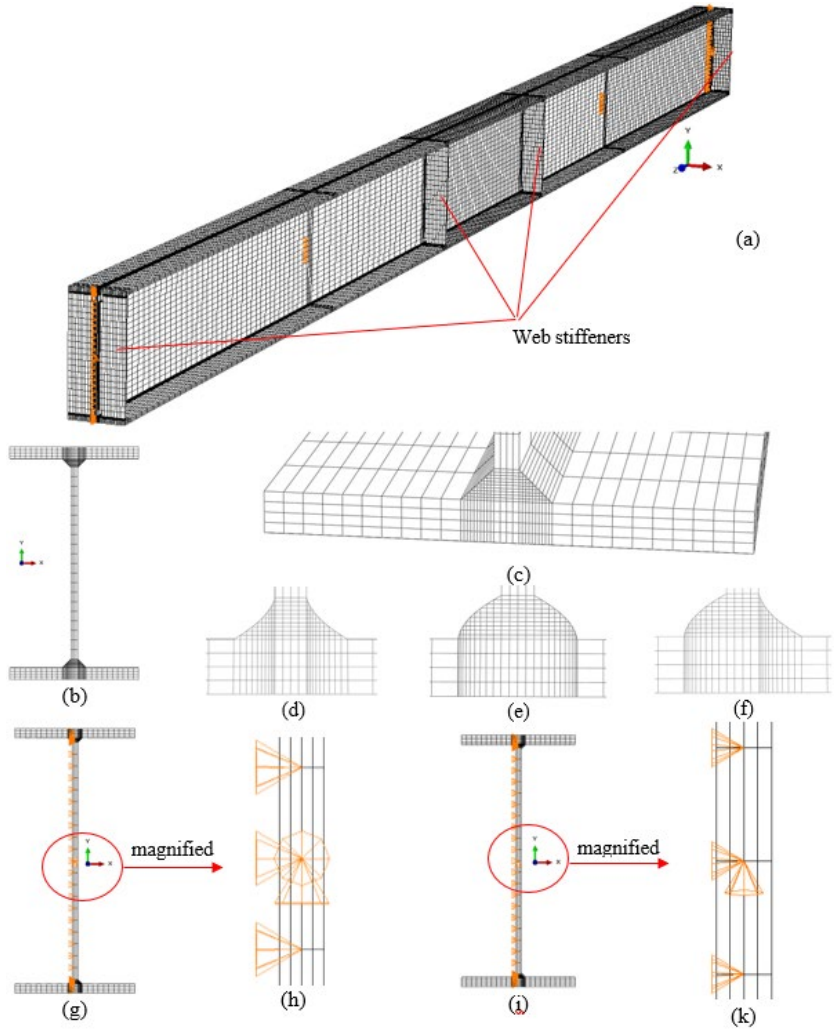

Fig. 7**.** Mesh generations (a) 3D view, (b) cross-section view, (c) magnified 3D view of bottom flange with line weld shape, (d, e, f) concave, convex and mixed weld shapes, (g, i) pin and movable supports at Points A and B, and (h, k) magnified views of the pin and movable supports

3.2 Model verifications

The moment-deflection relationships obtained from the present numerical study are validated against those of design specifications [1, 2] and experimental results [20]. The first verification is conducted for Beam SS00. Fig. 8 presents a comparison of the moment-vertical deflection relationship of Beam SS00 as obtained from the present study and the plastic moment M_p obtained from AISC A360-22 [1] or EC 3 [2]. It is observed that the peak moment (or moment resistance) based on the present study is 600.0 kN.m, while M_p is 597.7 kN.m, a slight difference of 0.4%. As defined in Table 2, Beam SS00 does not consider the effect of both residual stresses and initial-out-of-straightness and thus the system can develop to the plastic moment.

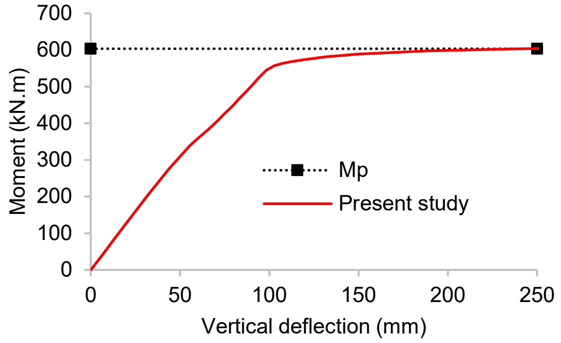

Fig. 8. Comparison of the present solution against the plastic moment M_p for the case of beam SS00

The second validation is conducted for Beam SS02, which was experimentally tested by Le et al. [20]. Fig. 9a,b present the comparisons of the moment-vertical deflection and moment-lateral displacement as obtained from the experimental results [20] and the present study. It is observed that the curves based on the present study are in agreement with those of the experimental study. Also, the peak moment based on the experimental study is 509.0 kN.m, while that of the present study is 504.0 kN.m, corresponding to a difference of only 1.0%. The peak deflection of the experiment occurs at a vertical deflection of 90.5 mm and at a lateral displacement of 8.0 mm, while that of the present study is at a vertical deflection of 94.0 mm and a lateral displacement of 8.0 mm. These indicate that the present numerical results can excellently capture the inelastic deformations and moment resistances of the beams under the effects of the initial imperfections.

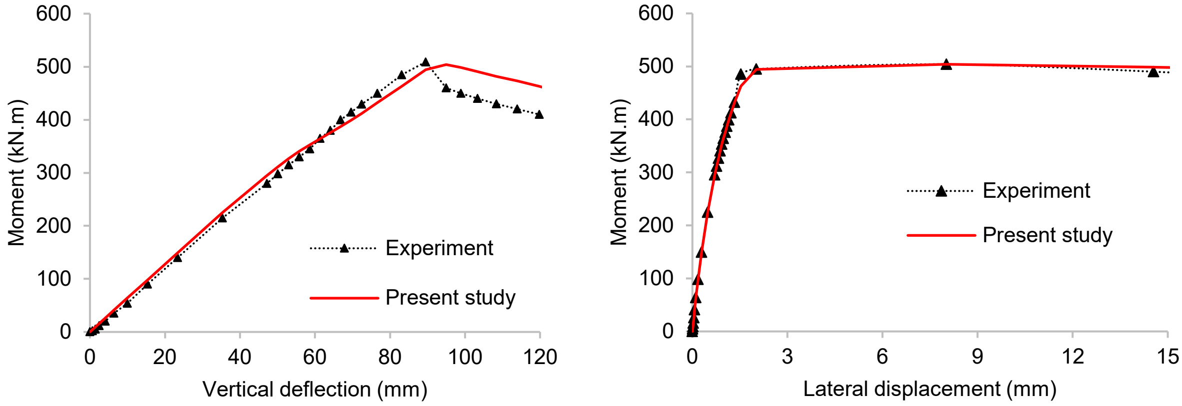

(a) (b)

Fig. 9: Comparisons of the moment-deflection relationships obtained from the present study and experiment results [20] for Beam SS02

4 Effects of the initial imperfection shapes of welds, braces, and out-of-straightness on the inelastic moment resistances of the systems

The numerical solution procedure developed in the present study is applied to investigate the effect of the initial imperfection shapes of welds, braces, and out-of-straightness on the inelastic LTB moment resistances of 37 Beams (as defined in Table 2). Three investigations are separately discussed in the following, in which Investigation 1 is for the effects of the weld shapes, Investigation 2 is for the effects of the lateral bracing conditions, and Investigation 3 is for the effects of the initial out-of-straightness shapes.

4.1 Investigation 1. The effects of the weld shapes

The effects of linear, concave, convex and mixed weld shapes (as defined in Fig. 2b1-b4, Fig. 5, Fig. 7) on the system moment resistances can be observed through the analyses of Beams SS02, SS04, SS05 and SS06 (in which SS02 is based on ReS1, SS04 is based on ReS2, SS05 is based on ReS3, and SS06 is based on ReS4). The moment-deflection relationships of the beams are obtained from the present numerical solution and they are presented in Fig. 10. A magnified picture of the peak moment zone is also overlaid in the figure to have a more obvious view. As observed, the relationships of all the Beams are almost indifferent. The moment resistance of Beam SS02 is 483.7 kN.m, that of Beam SS04 is 484.4 kN.m, and that of both Beams SS05 and SS06 is 484.8 kN.m. If the resistance of Beam SS02 is considered as a reference value, the moment of Beam SS04 is 0.2% higher, and those of Beams SS05 and SS06 are 0.3% higher. As a result, the moments of the Beams with the concave, convex or mixed weld shapes (e.g., SS04, SS05, SS06) are not really different to those of the Beam with a linear weld shape (e.g., SS02). The neglibile differences can be explained by the fact that the weld shapes have the mechanical properties (e.g., cross-sectional area and moment of inertials) much smaller than those of the whole steel beam cross-section.

Although the effect of weld shapes on the moment resistances are negligible, the system responses are considerably dependent on the residual stresses. Beam SS01 includes ReS1 residual stresses but it neglects the initial out-of-straightness shape. The moment resistance of SS01 is 529.9 kN.m, which is 9.6% higher than the moment resistance of Beam SS02.

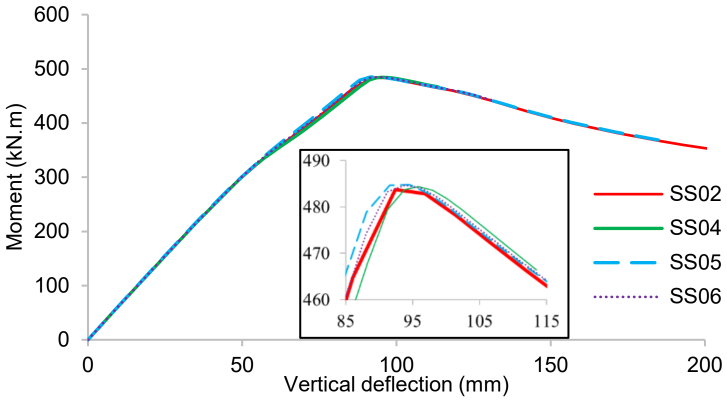

Fig. 10: Effects of residual stress conditions (ReS1, ReS2, ReS3, ReS4) on the system moment resistances

4.2 Investigation 2. Effect of lateral bracing conditions

Fig. 11a-d present the comparisons of the moment-deflections of the beams under the effect of different bracing conditions, in which Fig. 11a presents the comparison for Beams SS13, SS15, SS17 and SS19 with CS1 section under the same ReS1 and IMM1 but different bracing conditions BS1, BS2, BS3 and BS4. Similar comparisons in Fig. 11b, c, d are respectively performed for Beams SS21, SS23, SS25 and SS27 with CS2 section, for Beams SS02, SS07, SS09 and SS11 with CS3 section, and for Beams SS29, SS31, SS33, and SS35 with CS4 section.

As observed from Fig. 11a, the moment resistances of the beams are influenced by the bracing conditions. The moment resistance of Beam SS13 with BS1 (i.e., the web height is laterally braced, $h_{br} = h_w$) is 569 kN.m, that of Beam SS15 with BS2 (i.e., $h_{br} = h_w/2$) is reduced to 555 kN.m, that of SS17 with BS3 (i.e., $h_{br} = h_w/4$) is 534 kN.m, and that of beam SS19 with BS4 (i.e., $h_{br} = h_w/8$) is 360.2 kN.m. If the moment resistance of Beam SS13 is taken as the reference value, that of Beam SS15 is 2.5% lower, that of Beam SS17 is 6.2% lower, while that of Beam SS19 is 36.8%. The margin difference of the buckling moments between Beams SS13 and SS15 indicate that the moment resistances of the beams with a half of the web height laterally braced can approximately equals to those with the whole web height laterally braced. However, the large differences between SS13 and SS17 or SS13 and SS19 show that when the bracing height is not big enough, the moment resistance of the beams will be significantly reduced. Similar observations can be obtained from Fig. 11b, c for the beams with CS2 and CS3 sections. The reductions of the moment resistances under the different bracing conditions can be explained by observing the beam deformations as presented in Fig. 12. For Beams SS13 and SS15 with $h_{br} = h_w$ and $h_{br} = h_w/2$ (Fig. 12a1, a2), it is observed that the cross-sections at Points B and C only have vertical displacements, no twisting angles at the cross-sections are found. For Beams SS17 with $h_{br} = h_w/4$ (Fig. 12b1, b2), the cross-sections at Points B and C mainly have vertical displacements but they are slightly twisted. For Beams SS19 with $h_{br} = h_w/8$ (Fig. 12c1, c2), the cross-sections at Points B and C have high vertical displacements and big twisting angles, the beam deformation is probably approaching to that of simply supported beams without having lateral bracings at Points B and C.

Fig. 11d presents the moment-deflection relationships of Beams SS29, SS31, SS33, and SS35 with CS4 cross-section. The moment resistance is obtained as 260.1 kN.m for Beam SS29 (with the whole web is laterally braced), that is 249.7 kN.m for Beam SS31 (with one half of the web is braced), that is 249.3 kN.m for Beam SS33 (with one fourth of the web is braced) and that is 248.6 kN.m for Beam SS35 (with one eighth of the web is braced). If the resistance of Beam SS29 is taken as the reference value, that of SS31 is 4.0% lower, that of SS33 is 4.2% lower, and that of SS35 is 4.4% lower. The small differences between the resistances indicate that the effects of the different lateral bracing conditions on the moments are not considerable. In fact, local buckling deformations on the flanges have been observed for all of the Beams, as presented in Fig. 13. Because the cross-sections considered in Beams SS29, SS31, SS33, and SS35 is CS4 that was classified as slender flanges and a slender web (or class 4 section), such local buckling deformations have occurred in the analyses.

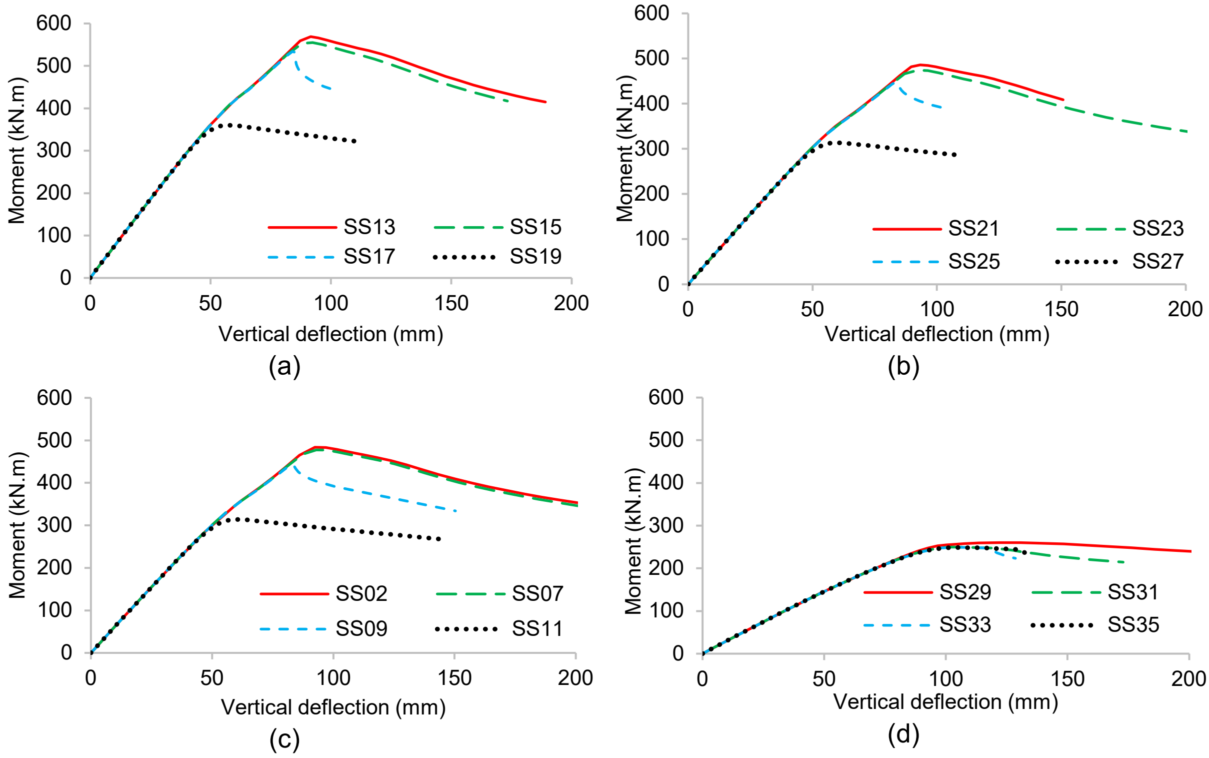

Fig. 11: Effects of lateral bracing conditions (BS1, BS2, BS3, BS4) on the moment-deflection relationships of the beams with (a) CS1, (b) CS2, (c) CS3 and (d) CS4 cross-sections

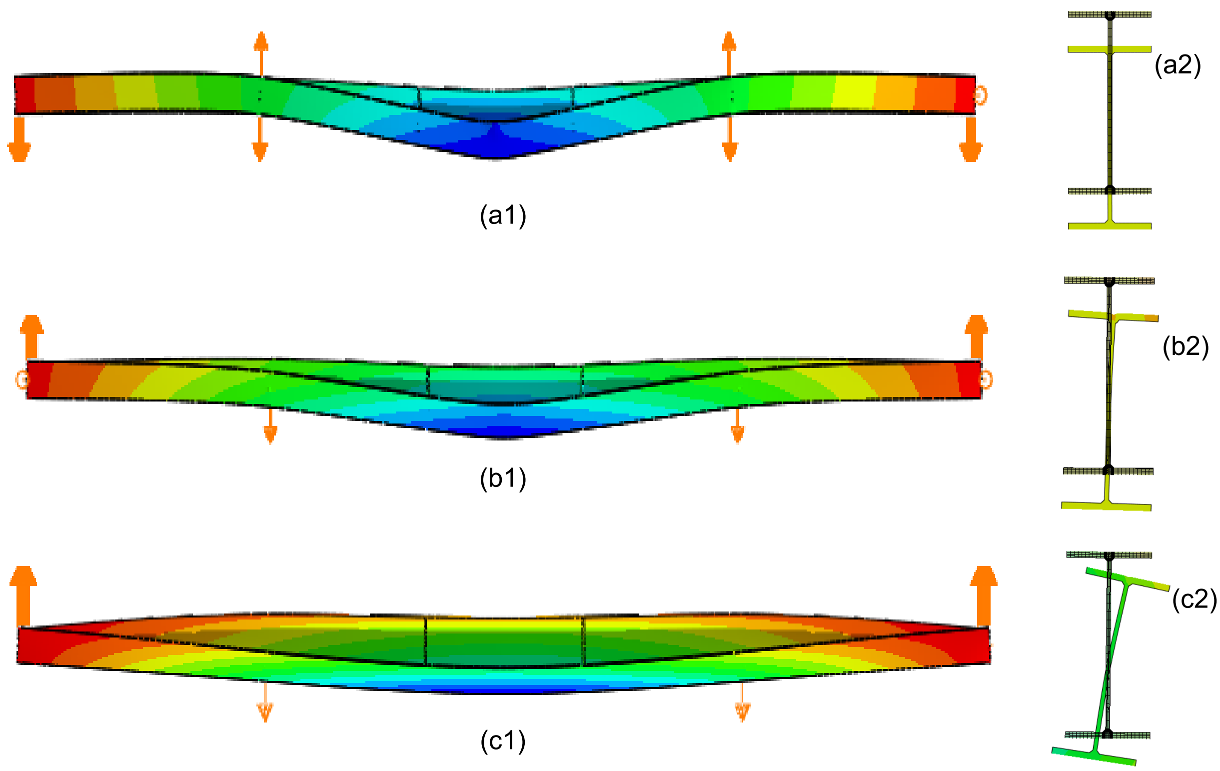

Fig. 12: Effects of lateral bracing conditions on the beam deformations: plan and section views of (a1, a2) Beams SS13 or SS15, (b1, b2) Beam SS17, and (c1, c2) Beam SS19

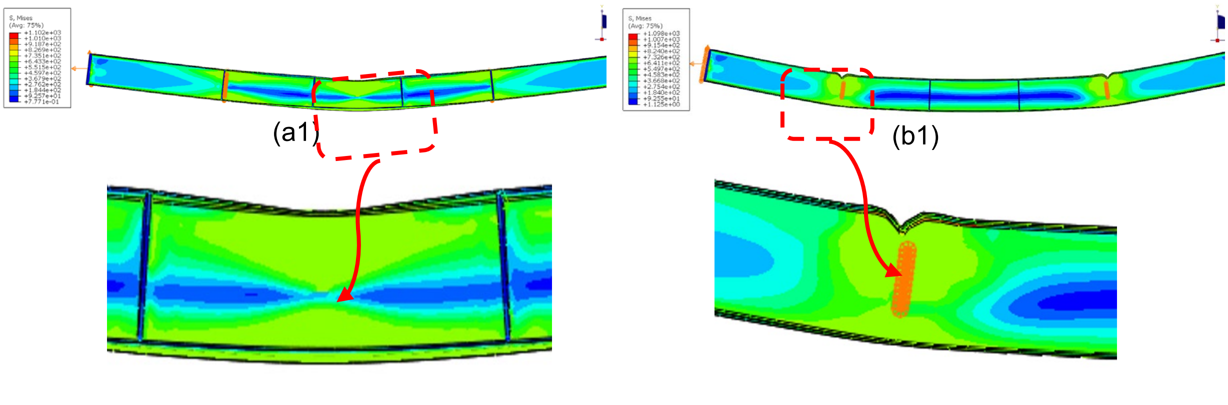

Fig. 13: Local buckling deformations in the beams with slender sections: (a1, b1) elevation views of SS29 and SS31 beams, (a2, b2) magnified views

Investigation 3. Effect of the initial out-of-straightness shapes

The initial out-of-straightness of steel beams has a strong effect on their moment resistances [2,40]. Such an initial imperfection shape may be obtained by adjusting four governing displacement fields at each cross-section, those are a lateral displacement, a twisting angle, a lateral slope and a warping deformation [2,13]. Most specifications and previous research works (e.g., [2,13,19,20,40-45]) assumed that the initial imperfection shape was based on the first elastic lateral torsional buckling mode with a maximum out-of-straightness amount of $L_0/1000 = 3.0\,mm$ (e.g., Fig. 2d1). The lateral displacement and the torsional angle were assumed as a half cycle of a sine wave. In fact, the initial imperfection may have different forms, for example of a form of the second lateral torsional buckling mode (with a full sine wave cycle of the governing displacements, for example of Fig. 2d2). To investigate the effect of such imperfection mode shapes with the same magnitude of amplitude of $L_0/1000 = 3.0\,mm$ (Fig. 2d1,d2) on the inelastic moment resistances of the beams, the present part compares and discusses the moment-deflection relationships of 8 pairs of beams, those are SS13 and SS14 beams with CS1 cross-section and BS1 bracing conditions (Fig. 14a), SS19 and SS20 beams with CS1 cross-section and BS4 bracing conditions (Fig. 14a), SS21 and SS22 beams with CS2 cross-section and BS1 bracing conditions (Fig. 14b), SS27 and SS28 beams with CS2 cross-section and BS4 bracing conditions (Fig. 14b), SS02 and SS03 beams with CS3 cross-section and BS1 bracing conditions (Fig. 14c), SS11 and SS12 beams with CS3 cross-section and BS4 bracing conditions (Fig. 14c), SS29 and SS30 beams with CS4 cross-section and BS1 bracing conditions (Fig. 14d), and SS35 and SS36 beams with CS4 cross-section and BS4 bracing conditions (Fig. 14d).

For the moment-deflection relationships of SS13 and SS14 beams (Fig. 14a), the moment resistance of SS13 is 569.0 kN.m, and that of SS14 is 620.7 kN.m, a difference of 9.1%. For the moment-resistances of SS19 and SS20 beams (Fig. 14a), the moment resistance of SS19 is 360.2 kN.m, and that of SS14 is 542.3 kN.m, a difference of 50.6%. It is thus observed that the effects of the initial out-of-straightness shapes on the moment resistance of the beams are significant. Fortunately, the moment resistances of the beams with IMM1 (i.e., the imperfection shape is taken from the first lateral torsional buckling mode) are lower than those with IMM2 (i.e., the imperfection shape is taken from the second lateral torsional buckling mode). Similar observations can be achieved for the Beams with CS2 (Fig. 14b) and CS3 (Fig. 14c) sections.

For the moment-deflection relationships of SS29 and SS30 beams (Fig. 14d), the moment resistance of SS29 is 260.1 kN.m, and that of SS30 is 267.5 kN.m, a difference of 2.8%. For the moment-resistances of SS35 and SS36 beams (Fig. 14d), the moment resistance of SS35 is 248.6 kN.m, and that of SS36 is 250.1 kN.m, a difference of 0.6%. Obviously, the effect of initial out-of-straightness shape based on IMM1 or IMM2 on the moment resistances of the beams with slender CS4 sections are not considerable. As discussed, the resistances of the beams are based on the local buckling of the slender flanges, as observed in Fig. 13.

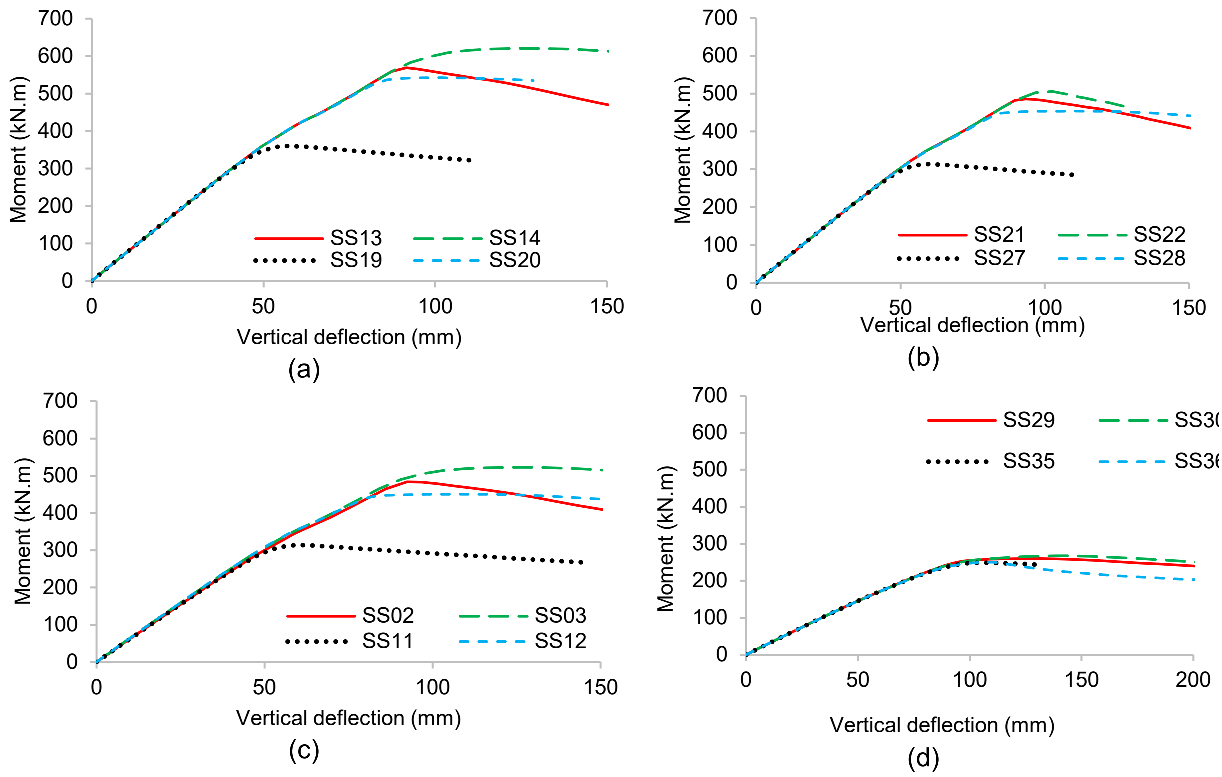

Fig. 14: Effects of the initial out-of-straightness conditions (IMM1, IMM2) on the moment resistances of the beams with (a) CS1, (b) CS2, (c) CS3 and (d) CS4 cross-sections

5 Design considerations for the moment resistances of AISC and EC 3 specifications

5.1 Summary of the resistance evaluations in AISC [1]

Table 6 presents the section classifications based on AISC [1] specification. In AISC [1], λ is taken as $b_f/2t_f$ for the flange while it is h_w/t_w for the web, λ_p and λ_r are the section limits. If $\lambda \le \lambda_p$ and the flange is continuously connected to the web, the element is compact; if $\lambda_p < \lambda \le \lambda_r$, the element is noncompact; and if $\lambda > \lambda_r$, the element is slender.

Table 6: Sectional classifications of AISC A360-22 [1] specification

Element	**λ**	**λp**	**λr**
Flange	$\dfrac{b}{2t_f}$	$0,38\sqrt{\dfrac{E}{F_y}}$	$0,95\sqrt{\dfrac{k_c E}{F_L}}$
Web	$\dfrac{h_w}{t_w}$	$3,76\sqrt{\dfrac{E}{F_y}}$	$5,7\sqrt{\dfrac{E}{F_y}}$

where *E* is the modulus of elasticity of steel, F_y is the specified minimum yield stress of the steel, k_c is not less than 0,35 nor greater than 0,76:

$$k_c = \frac{4}{\sqrt{h/t_w}} \tag{1}$$

F_L = nominal compression flange stress above which the inelastic buckling limit states apply. When $S_{xt}/S_{xc} \ge 0,7$ then $F_L = 0,7F_y$ and when $S_{xt}/S_{xc} < 0,7$ then $F_L = F_y S_{xt}/S_{xc} \ge 0,5F_y$, in which S_{xt} is the elastic section modulus referred to tension flange, and S_{xc} is the elastic section modulus referred to compression flange.

The evaluation of the moment resistance M_n based on AISC [1] is summarized in Table 7. It is dependent on the relationship between the unbraced length L_b and limit lengths L_p and L_r. For the beams with slender sections, it also depends on the compression flange local buckling moment. In Table 7, the following parameters are defined: r_y is the radius of gyration about $y-$axis; J is the St. Venant torsional constant, I_y is the flexural moment of inertia about the weak axis of the section, S_x is elastic section modulus taken about the *x*-axis, and h_o is the distance between the flange centroids. where $r_{ts}^2 = \sqrt{I_y C_w}/S_x$ with $I_y =$ moment of inertia about the weak axis of the section, C_w is the warping torsional constant of the section; c is the coefficient, for doubly symmetric I-shapes $c = 1$. $r_t =$ effective radius of gyration for lateral-torsional buckling:

$$r_t = \frac{b_{fc}}{\sqrt{12\left(1+\frac{a_w}{6}\right)}} \tag{2}$$

$$a_w = \frac{h_c t_w}{b_{fc} t_{fc}} \leq 10 \tag{3}$$

in which $b_{fc} =$ width of compression flange; $t_{fc} =$ thickness of compression flange; $t_w =$ thickness of web; $h_c =$ twice the distance from the centroid to the following: the nearest line of fasteners at the compression flange or the inside face of the compression flange when welds are used, for built-up sections. The moment gradient factor C_b is evaluated as $C_b = A.B^{2y_P/h}$, where $A = 1 + \left[L_1/(2L_1 + L_0)\right]^2$, $B = 1,0 - 0,465W^2 + 1.636W$, and $W = (\pi/L)\sqrt{EC_w/GJ}$.

Table 7: Evaluation of the moment resistances based on AISC [1] specification

Sections with compact webs and compact or non-compact flanges	Sections with slender webs and slender flanges
$L_p = 1,76 r_y \sqrt{\frac{E}{F_y}}$; $L_r = 1,95 r_{ts} \frac{E}{0,7F_y} \sqrt{\frac{Jc}{S_x h_o} + \sqrt{\left(\frac{Jc}{S_x h_o}\right)^2 + 6,76\left(\frac{0,7F_y}{E}\right)^2}}$	$L_p = 1,1 r_t \sqrt{\frac{E}{F_y}}$; $L_r = \pi r_t \sqrt{\frac{E}{0,7F_y}}$
$L_b \leq L_p : M_n = M_p = F_y Z_x$ $L_p < L_b \leq L_r :$ - Compact web, compact flange: $M_n = C_b\left[M_p - (M_p - 0,7F_y S_x)\left(\frac{L_b - L_p}{L_r - L_p}\right)\right] \leq M_p$ - Compact web, non-compact flange: $M_n = M_p - \left(M_p - 0,7F_y S_x\right)\left(\frac{\lambda - \lambda_{pf}}{\lambda_{rf} - \lambda_{pf}}\right)$ with $\lambda = b_f/2t_f$; $\lambda_{pf} = \lambda_p$; $\lambda_{rf} = \lambda_r$; $L_b > L_r :$ $M_n = S_x \frac{C_b \pi^2 E}{\left(L_b/r_{ts}\right)^2} \sqrt{1 + 0,078 \frac{Jc}{S_x h_o}\left(\frac{L_b}{r_{ts}}\right)^2} \leq M_p$	$L_b \leq L_p : M_n = M_p = R_{pg} F_y S_{xc}$ $R_{pg} = 1 - \left[\frac{a_w\left(\frac{h_c}{t_w} - 5,7\sqrt{\frac{E}{F_y}}\right)}{\left(1200 + 300a_w\right)}\right] \leq 1,0$ $L_p < L_b \leq L_r :$ $M_n = R_{pg} C_b \left[F_y - (0,3F_y)\left(\frac{L_b - L_p}{L_r - L_p}\right)\right] S_{sc} \leq M_p$ $L_b > L_r :$ $M_n = R_{pg} \frac{C_b \pi^2 E}{\left(L_b/r_t\right)^2} S_{sc} \leq M_p$ Compression flange local buckling moment: $M_n = R_{pg} \frac{0,9Ek_c}{\left(\frac{b_f}{2t_f}\right)^2} S_{xc}$

5.2 Summary of the resistance evaluations in EC3 [2]

Table 8 presents the section classifications based on EC3 [2] specification. In EC3 [2], $c_f = (b - t_w - 2t_{we})/2t_f$, $c_w = (h_w - 2h_{we})/t_w$ and $\varepsilon = \sqrt{235/F_y}$. The section can be classified as class 1, 2, 3 or 4 based on the relations defined in Table 8.

Table 8: Sectional classifications of EC3 [2] specifications

Element	EC3 [2]			
	Class 1	Class 2	Class 3	Class 4
Flange	$\frac{c_f}{t_f} \leq 9\varepsilon$	$9\varepsilon < \frac{c_f}{t_f} \leq 10\varepsilon$	$10\varepsilon < \frac{c_f}{t_f} \leq 14\varepsilon$	$\frac{c_f}{t_f} > 14\varepsilon$

Web	$\frac{c_w}{t_w} \leq 72\varepsilon$	$72\varepsilon < \frac{c_w}{t_w} \leq 83\varepsilon$	$83\varepsilon < \frac{c_w}{t_w} \leq 124\varepsilon$	$\frac{c_w}{t_w} > 124\varepsilon$

In EC3 [2] specification, the design buckling resistance moment is evaluated as:

$$M_n = \frac{\chi_{LT} W_y F_y}{\gamma_{MI}} \tag{4}$$

where γ_{MI} is a safety factor and it is assumed as $1,0$ in the present study; W_y is the appropriate section modulus that can be obtained as: $W_y = W_{pl,y}$ for Class 1 or 2 cross-sections, $W_y = W_{el,y}$ for Class 3 cross-sections, and $W_y = W_{eff,y}$ for Class 4 cross-sections. χ_{LT} is the reduction factor for the lateral-torsional buckling and it is evaluated as:

$$\begin{cases} \chi_{LT} = \dfrac{1}{\phi_{LT} + \sqrt{\phi_{LT}^2 - \beta \overline{\lambda}_{LT}^2}} \leq 1 \\ \chi_{LT} \leq \dfrac{1}{\overline{\lambda}_{LT}^2} \end{cases} \tag{5}$$

where $\phi_{LT} = 0,5\left[1 + \alpha_{LT}\left(\overline{\lambda}_{LT} - \overline{\lambda}_{LT,0}\right) + \beta \overline{\lambda}_{LT}^2\right]$; in which α_{LT} is an imperfection factor and it is taken as 0.49 for the buckling curve of *c*, or 0.76 for the buckling curve of *d*. The buckling curve is c if the limits of h/b (where $h = h_w + 2t_f$) ≤ 2, and it is d if h/b>2. Also,$\overline{\lambda}_{LT,0} = 0.4$ and $\beta = 0.75$ are given. And,

$$\overline{\lambda}_{LT} = \sqrt{\frac{W_y F_y}{M_{cr}}} \tag{6}$$

in which M_{cr} is the elastic lateral torsional buckling moment and it can be evaluated as:

$$M_{cr} = C_1\left(\frac{\pi^2 EI_z}{L^2}\right)\left(\sqrt{\frac{I_w}{I_z} + \frac{L^2 GI_T}{\pi^2 EI_z} + \left(C_2 z_g\right)^2} - C_2 z_g\right) \tag{7}$$

where C_1 is a coefficient accounting for the moment distribution gradient, C_2 is a coefficient accounting for the effect of load height position. For the present problems, $C_1 = 1,040$ and $C_2 = 0,431$ are selected [2]; z_g is the distance between the point of load application and the shear center (i.e., sectional centroid in the present problem); I_w is the warping torsional constant of the section; I_T is the torsional constant; and I_z is the moment of inertia about the weak axis of the section.

5.3 Comparisons of the moment resistances obtained from AISC [1], EC3 [2] and the present solutions

The Beams from SS00 to SS36 given in Table 2 are considered for the comparisons. As presented in Sections 5.1 and 5.2 above, the AISC [1] and EC3 [2] specifications have strict requirements for the moment resistance designs of the unbraced segments of the steel beams with different cross section classifications. However, the effects of initial imperfection shapes of braces, welds and out-of-straightness on the moment resistances seem not to be covered by the design equations. Besides, the system is laterally braced at the cross-section where load P is applied at its top flange (Fig. 2a). In such a case, it may challenges engineers to evaluate the moment resistances of the systems with or without a consideration of the bracing conditions and load height positions. Also, the design guides of the EC3 [2] specification applied for the beams from SS0 to SS36 lead to a selection of the buckling curve *d* for the moment resistances. This implies that the EC3 [2] – based solutions may assume that the beams have a design value of initial local bow imperfection of $e_0 = L_0/150 = 20mm$. This value is significantly higher than the out-of-straightness magnitude of $L_0/1000 = 3.0\,mm$ applied for the beams in the present numerical solution (the magnitude is also required by AISC [1]). As a result, the EC3 solutions may be more conservative than the present solutions. This part will clarify the issues by comparing the moment resistances obtained from AISC [1] and EC3 [2] specifications against those of the present numerical solutions. Based on the parameters given in Table 2, the moment resistances of Beams SS0 to SS36 can be evaluated and they are presented in Table 9.

For the beams from SS13 to SS20 with CS1 cross-section, it is observed that the moment resistance evaluated by AISC [1] specification is 441.3 kN.m, that based on EC 3 [2] is 311.3 kN.m. The solution based on EC3 is more conservative than the AISC solution. It can be observed that the moment resistances based on the specifications are insensitive to the initial imperfection shapes of braces, residual stresses and out-of-straightness. However, the moment resistances based on the present numerical solutions are varied in a range from 360.2 kN.m (beam SS19) to 620.7 kN.m (Beam SS14), a difference of 72.3%. Besides, the moment resistances of the beams with BS1, BS2, and BS3 bracing conditions (except Beam SS19) based on AISC [1] and EC3 [2] are considerably smaller than those of the numerical results. For example, the moment resistance of Beam SS13 predicted by the present numerical solution is 569.0 kN.m, that is 1.4 times higher than the resistance of the AISC [1] and 1.8 times higher than that of the EC3 [2]. As a result, the moment resistances based on the AISC [1] and EC3 [2] are relatively conservative for the moment evaluations. For Beam SS19 (with BS4 bracing conditions), the moment resistance of the numerical solution is 360.2 kN.m, that is lower than the AISC solution, but it is higher than the EC3 [2] solution. This indicates that the design treatment based on AISC may be not conservative enough, and that the EC3 [2] solution can ensure that the design is safe. The overestimation of the AISC may be originated by the fact that the above AISC solutions have not considered the effect of the least bracing condition (i.e., BS 4 - a one eighth of the web height was braced, as defined in Section 2), while the present numerical solution has captured this condition. In such cases, it is recommended to re-evaluate the moment resistances of the AISC by accounting for the effects of the non-bracing conditions (i.e., lateral braces at B and C are not considered) and/or the load height positions (i.e., load is applied on the top flange). Specifically, the moment resistance is 196.6 kN.m if the load heigh effect is captured and it is reduced to 81.2 kN.m if both of the effects are considered. However, such treatments have led to very conservative results of the AISC solution compared against the present numerical results.

Table 9: Evaluations of the moment resistances (kNm) based on AISC [1], EC3 [2] specifications and the present numerical results

Beam #	Cross-section	AISC [1]	EC3 [2]	Numerical results
SS13	CS1	441.3	311.3	569.0
SS14				620.7
SS15				555.0
SS16				614.8
SS17				534.0
SS18				600.8
SS19		441.3 (196.6*), (81.2**)	311.3	360.2
SS20				542.3
SS21	CS2	357.9	255.0	485.9
SS22				505.9
SS23				474.2
SS24				499.5
SS25				447.6
SS26				486.0
SS27		357.9 (156.1*), (58.3**)	255.0	313.6
SS28				453.9
SS00	CS3	356.6	242.0	597.1
SS01				529.9
SS02				483.7
SS03				522.6
SS04				484.4
SS05				484.8
SS06				484.8
SS07				477.4
SS08				489.6
SS09				442.9
SS10				481.6
SS11		356.6 (155.4*), (57.6**)	242.0	313.9
SS12				450.4
SS29	CS4	62.1	77.0	260.1
SS30				267.5
SS31				249.7

SS32				250.7
SS33				249.3
SS34				250.3
SS35				248.6
SS36				250.1

* Value accounting for the effect of load height position

** Value accounting for the effects of both load height position and non-bracing conditions

For the beams with CS2 cross-section (i.e., SS21 to SS28) or the beams with CS3 cross-sections (i.e., SS00 to SS12), it is again observed that the moment resistances based AISC [1] and EC3 [2] are constants, while those based on the present numerical solution strongly depends on the initial imperfection effects. Excepts Beams SS27 and SS11, the resistances of AISC [1] and EC3 [2] solutions are smaller (i.e., more conservative) than those of the present numerical solutions. For Beams SS27 and SS11, it is again recommended to consider the effects of load height and/or non-bracing conditions in the AISC solutions to obtain a conservative design for the moment resistances.

For the beams with CS4 cross-sections (i.e., Beams from SS29 to SS36), the moment resistance based on AISC is 62.1 kN.m and that based on EC3 is 77.0 kN.m, while those based on the present numerical results are ranged from 248.6 kN.m to 267.5 kN.m. All solutions are based on the failure mode of local flange buckling. Therefore, the present solution are 4.0-4.3 times higher than the AISC solution and 3.2-3.5 times higher than the EC3 solution. This indicates that the current design guide for beams with slender cross-sections of AISC and EC3 are conservative solutions regardless of effects of the initial imperfection shapes of welds, braces, and out-of-straightness.

6 Conclusion

The present study successfully performed a numerical procedure to obtain the inelastic resistances of steel beams with the initial imperfection shapes of welds, lateral braces, and out-of-straightness. The numerical procedure was based on three types of analyses, of which the first one was a nonlinear coupled temperature - displacement analysis of the structure under a welding process to obtain residual stresses, the second one was an elastic buckling analysis to obtain initial out-of-straightness through an adjustment of the first or the second elastic lateral torsional buckling modes, and the third one was a nonlinear plasticization analysis to obtain the inelastic resistances of the system under the effects of bracing, residual stresses (taken from the first analysis) and the initial out-of-straightness (taken from second analysis). The geometric and material nonlinearities were captured by the present numerical solutions. The convergent deformations and moments based on the present numerical solutions were successfully validated against experimental results and specification solutions. Thirty seven practical beams, denoted from SS0 to SS36, were proposed to quantify the effects of the initial imperfection shapes of welds, bracing heights, out-of-straightness and sectional classes on the system deformations and moment resistances.

For the beams with compact or noncompact flanges and webs, key conclusions have been obtained as follows.

1) As observed in Investigation 1, residual stresses had a considerable effect on the moment resistances of the steel beams, this was evidenced by a difference of 9.6% between the moment resistances of the Beam with no imperfection (SS00) and the Beam with residual stresses (SS01). However, the moment resistances of the Beams with concave, convex or mixed weld shapes were marginally different to that of the Beams with a linear weld shape. The difference of the moment resistances of between the Beams was within 0.3%.

2) As observed in Investigation 2, the moment resistances of the beams with BS1 bracing conditions (i.e., the web depths were fully braced) were almost equal to those with BS2 (i.e., the web depths were half braced). In contrast, the moment resistances of the beams with BS3 and BS4 bracing conditions (i.e., one fourth and one eighth of the web depths were braced, respectively) were significantly reduced. The difference of the moment resistances of Beams SS13 and SS19 was 36.8%, and that of Beams SS16 and SS20 was 12.6%. The beams with BS3 and BS4 braces were unable to fully restraint the twisting deformations at the braced cross-sections.

3) As observed in Investigation 3, the moment resistances of the beams with initial out-of-straightness based on the first elastic LTB mode were from 9.1% to 50.6% different to those based on the second elastic LTB mode.

4) The moment resistances of the Beams with BS1, BS2 and BS3 bracing conditions evaluated by the present numerical study were considerably higher than those evaluated by the AISC and EC 3 specifications. However, the moment resistances of the Beams with BS4 bracing systems (e.g., SS11, SS19, SS27) evaluated by the present study were lower than those of the AISC specification, but they were higher than the EC 3 solutions. In this case, the present study recommended to consider the effects of non-bracing conditions and/or the load height positions in the AISC solutions to obtain conservative designs of the moment resistances. The moment resistances based on the EC 3 solution were more conservative than those based on the AISC solutions and the present numerical solutions.

For the beams with slender flanges and webs, the following key conclusions have been achieved.

5) As observed in Investigations 1, 2 and 3, the moment resistances of the beams with slender sections were insensitive to the initial imperfection shapes of welds, braces and out-of-straightness, but they were failed by local buckling of the flanges.

6) The moment resistances of the beams with slender sections evaluated by the present numerical study were significantly higher than those evaluated by the AISC and EC 3 specifications. This indicated that the current design guide of AISC and EC3 specifications for beams with slender cross-sections under the initial imperfection effects of welds, braces, and out-of-straightness were relatively conservative.

Acknowledgement

This research was supported by Vietnam Ministry of Education and Training, Project B2023-GHA-06

References

[1] ANSI/AISC-360: Specification for structural steel buildings, American Institute of Steel Construction (AISC), Chicago, IL, 2022, 780 p.

[2] EN-1993, EUROCODE 3: Design of steel structures - Part 1-1: General rules and rules for buildings, 2005, 93p.

[3] THIEBAUD R. – LEBET J.P. – BEYER A. – BOISSONNADE N.: Lateral torsional buckling of steel bridge girders, Proceedings of the Annual Stability Conf,, Structural Stability Research Council Orlando, Florida, 2016, 19p.

[4] THIEBAUD R.: Lateral Torsional Buckling of Steel Bridges, 2014, Accessed on July 30th 2024 by the link: https://memento.epfl.ch/event/lateral-torsional-buckling-of-steel-bridges/.

[5] MEHRI H. – CROCETTI R.: Bracing of steel-concrete composite bridge during casting of the deck, Nordic Steel Construction Conference, Norway, 2012, 10p.

[6] SHEDBAL, N.: Lateral Torsional Buckling | Factors influencing LTB, 2017, Accessed on July 30th 2024 by the link: https://engineeringcivil.org/articles/civil-engineering/lateral-torsional-buckling-factors-influencing-ltb/.

[7] ELLWAND, O.: It could be weeks before source of buckling 102nd Avenue bridge girders is found: engineer, Edmonton journal, 2015, Accessed on July 30th 2024 by the link: https://edmontonjournal.com/news/local-news/it-could-be-weeks-before-source-of-buckling-102nd-avenue-bridge-girders-is-found-engineer.

[8] NAGARAJA RAO, N.R. – ESTUAR, F.R. – TALL, L.: Residual stresses in welded shapes, Fritz Laboratory Reports, 1963, pp. 93-105.

[9] ALPSTEN, G.A. – TALL, L.: Residual Stresses in Heavy Welded Shapes, Weld J. Res. Supl., 49, 1970, pp 93–105.

[10] DWIGHT, J.B. – WHITE, J.D.: Prediction of weld shrinkage stresses in plate structures. Preliminary Report, 2nd International Colloquium on Stability of Steel Structures, ECCS – IABSE, 1977, pp. 31-7.

[11] SKYTTEBOL, A., -JOSEFSON, B.L., -RINGSBERG, J.W.: Fatigue crack growth in a welded rail under the influence of residual stresses, Engineering Fracture Mechanics, 72, 2005, pp. 271–285.

[12] STRIDSMAN, R.E.: Residual stresses induced by welding in high performance steel, master's thesis, Lulea university of technology, Lulea, Sweden, 2018, 105 p.

[13] VICAN, J. – GOCÁL, J. – ODROBINAK, J. – KOTES, P.: Existing steel railway bridges evaluation, Civil and Environmental Engineering, 12, 2016, pp. 103-110.

[14] KABIR, M.I. – BHOWMICK, A.K.: Lateral torsional buckling of welded wide flange beams. Proceedings of the annual stability conference, Structural Stability research council, Orlando, Florida, 2016, 14 p.

[15] ROSSI, A. – SAITO, D.H. – MARTINS, C.H.: The influence of structural imperfections on the LTB strength of I-beams, Structures, 29, 2021, pp. 1173-1186.
[16] TARAS, A.: Contribution to the Development of Consistent Stability Design Rules for Steel Members. TU Graz, 2010, 331 p.
[17] BARTH, K.E. – WHITE, D.W.: Finite element evaluation of pier moment-rotation characteristics in continuous-span steel I Girders, Engineering Structures, 2019, 98, pp. 761–78.
[18] SUBRAMANIAN, L. – WHITE, D.W.: Resolving the disconnects between lateral torsional buckling experimental tests, test simulations and design strength equations, J Constr Steel Res, 128, 2017, pp. 321–34.
[19] BOISSONNADE, N., -SOMJA, H.: Influence of imperfections in FEM modeling of lateral torsional buckling, Proceeding Annu. Stab. Conf. Struct. Stab. Res. Counc, 2012, pp. 1–15.
[20] LE, T. – BRADFORD, M.A., -LIU, X., -VALIPOUR, H.R.: Buckling of welded high-strength steel I-beams, Journal of Constructional Steel Research, 168, 2020, pp. 105938.
[21] TRAHAIR, N.S., -BRADFORD, M.A., -NETHERCOT, D.A., GARDNER, L.: The behaviour and design of steel structures to EC3. 4th edition, Taylor and Francis publisher, 1988, 513 p.
[22] TRAHAIR, N.S.: Inelastic buckling design of monosymmetric I-beams, Journal of Engineering Structures, 34, 2012, pp. 564-571.
[23] KUBO, M. – FUKOMOTO, Y.: Lateral torsional buckling of thin walled I beams, Journal of Structural Engineering, 114, 1988, pp. 841 – 855.
[24] NISHINO, F.– TALL, L. – OKUMURA, T.: Residual stress and torsional buckling strength of H and cruciform columns, Transaction of JSCE, 160, 1968, pp. 75-87.
[25] BAKER, K.A. – KENNEDY, D.J.: Resistance factors for laterally unsupported steel beams and biaxially loaded steel beam columns, Canadian J.of Civil Engineering, 11, 1984, pp. 1008 – 1019.
[26] ZIEMIAN, R.D.: Guide to stability design criteria for metal structures, John Wiley&Sons, 2010.
[27] ABEBE, D. – CHOI, J. – PARK, J.U.: Study on Inelastic Buckling and Residual Strength of H-Section Steel Column Member, International journal of steel structures, 15, 2014, pp. 365-374.
[28] KENNEDY, D.J.L. – ALY, M.G.: Limit states design of steel structures-performance factors, Canadian Journal of Civil Engineering, 7, 1980, pp. 45 – 77.
[29] WHITE, D.W. – JEONG, W.Y. – TOGAY, O.: Comprehensive Stability Design of Steel Members and Systems via Inelastic Buckling Analysis. 8th International Symposium on Steel Structures, Jeju, Korea, 2015, 13 p.
[30] COUTO C. – VILA REAL P.: Numerical investigation on the influence of imperfections in the lateral-torsional buckling of beams with slender I-shaped welded sections, Thin-Walled Struct., 145, 2019, pp. 106429.
[31] VALEŠ, J. – STAN, T.C.: FEM Modelling of Lateral-Torsional Buckling Using Shell and Solid Elements, Procedia Engineering, 190, 2017, pp. 464-471.
[32] PEZESHKY, P. – SAHRAEI, A. – MOHAREB, M.: Effect of bracing height on lateral torsional buckling resistance of steel beams. The CSCE con. on the Leadership in Sustainable Infrastructure, Vancouver, Canada, 2017, 10 p.
[33] DOU, C. – PI, Y.L.: Effects of Geometric Imperfections on Flexural Buckling Resistance of Laterally Braced Columns, ASCE Journal of Structural Engineering, 142, 2016, pp. 04016048.
[34] KORTIS J. – DANIEL, L. – SKARUPA, M. – DURATNY, M., Experimental model test of the laboratory model of steel truss structure, Civil and Environmental Engineering, 12, 2016, pp. 116-121.
[35] GOCAL, J. – HLINKA, R. – JOST, J. – BAHLEDA, F., Experimental analysis of stiffness of the reveted steel railway bridge deck members' joints, Civil and Environmental Engineering, 10, 2014, pp. 104-109.
[36] CANH, T.N. – JIHO, M. – VAN, N.L. – LEE, H.E.: Lateral-torsional buckling of I-girders with discrete torsional bracings, Journal of Constructional Steel Research, 66, 2010, pp. 170-177.
[37] CANH,T.N. – JIHO,M. – VAN,N.L. – LEE,H.E.: Flexural-torsional buckling strength of I-girders with discrete torsional braces under various loading conditions, Engineering Structures, 36, 2012, pp. 337-350.
[38] CANH,T.N. – JIHO,M. – VAN, N.L. – LEE, H.E.: Natural frequency for torsional vibration of simply supported steel I-girders with intermediate bracings, Thin-Walled Struc., 49, 2011, pp. 534-542.
[39] FOSTER, A.S.J. – GARDNER, L.: Ultimate behaviour of continuous steel beams with discrete lateral restraints, Thin-Walled Structures, 88, 2015, pp. 58-69.

[40] MOHAMMADI, E. – HOSSEINI, S.S., -ROHANIMANESH, M.S.: Elastic lateral-torsional buckling strength and torsional bracing stiffness requirement for monosymmetic I-beams, Thin-Walled Structures, 104, 2016, pp. 116-125.
[41] NAKAMURA, T.: Strength and Deformability of H-Shaped Steel Beams and Lateral Bracing Requirements, J Construct. Steel Research, 9, 1988, pp. 217-228.
[42] TONG, G.S. – CHEN, S.F.: Buckling of Laterally and Torsionally Braced Beams, J Construct. Steel Research, 11, 1988, pp. 41-55.
[43] PHE, P.V. – HUY, N.X.: Moment resistances of wide flange beams with initial imperfection and residual stresses, Journal of Materials and Engineering Structures, 7, 2020, pp. 651-658.
[44] PHE, P.V.: Enhancement of moment resistance of steel beams with initial imperfections and residual stresses by using stiffeners and GFRP plates, Journal of Materials and Engineering Structures, 7, 2020, pp. 659-667.
[45] BACHIRI, A. – BOUSSOUAR, A. – KABOUCHE, A. – SULEIMAN, M.F.: Numerical Study on Lateral Torsional Buckling of High Steel Welded I-Section Beam, First Arab Conference on Me. Eng., Biskra, Algeria, 2017, 6 p.
[46] YI, G.S.– KIM, J.K. – CHOI, B.H.: Inelastic moment-rotation response of 690 MPa Grade Steel I-section girders, International Journal of Steel Structures, 17, 2017, pp. 1667-2678.
[47] VIČAN, J. – FARBAK, M., Analysis of high-strength steel pin connection, Civil and Environmental Engineering, 16, 2020, pp. 276-281.